LETTER • OPEN ACCESS

Dissociative electron attachment cross sections for ro-vibrationally excited NO molecule and N¯ anion formation

View the article online for updates and enhancements.

Letter

Dissociative electron attachment cross sections for ro-vibrationally excited NO molecule and N⁻ anion formation

V Laporta[1],*[iD], I F Schneider[2,3][iD] and J Tennyson[4][iD]

[1] Istituto per la Scienza e Tecnologia dei Plasmi, CNR, Bari, Italy
[2] Laboratoire Ondes et Milieux Complexes, CNRS—Université Le Havre Normandie, Le Havre, France
[3] Laboratoire Aimé Cotton, CNRS—Université Paris-Saclay, ENS Cachan, Orsay, France
[4] Department of Physics and Astronomy, University College London, London, London WC1E 6BT, United Kingdom

E-mail: vincenzo.laporta@istp.cnr.it

Abstract
Motivated by the huge need for data for non-equilibrium plasma modeling, a theoretical investigation of dissociative electron attachment to the NO molecule is performed. The calculations presented here are based on the local-complex-potential approach, taking into account five NO⁻ resonances. Three specific channels of the process are studied, including the production of excited nitrogen atoms $N(^2D)$ and of its anions N⁻. Interpretation of the existing experimental data and their comparison with our theoretical result are given. A full set of ro-vibrationally-resolved cross sections and the corresponding rate coefficients are reported. In particular, a relatively large cross sections for N⁻ ion formation at low energy of the incident electron and for vibrationally excited NO target are predicted. Finally, molecular rotation effects are discussed.

Keywords: non-equilibrium plasma modeling, molecular physics, NO pollution, nitric oxyde, dissociative electron attachment, combustion processes, NO dissociation

(Some figures may appear in colour only in the online journal)

In a recent paper [1] we produced theoretical cross sections for the dissociative excitation of the nitric oxide (NO) molecule by electron impact. In order to supply further data for the non-equilibrium plasma modeling, and based on the same molecular data, in this letter we extend the calculations to its dissociative electron attachment (DA).

Although the NO molecule is only a minor constituent of Earth's upper atmosphere, it plays a major role in the infrared aurora borealis emissions [2] due to radiation coming from its vibrationally excited states, and in the energy transfers in the boundary layer of the plasma created in front of the spacecrafts entering in the planetary ionospheres [3–7]. Moreover, among the nitrogen oxide compounds N_xO_y, the NO molecule and its ions have the greater impact on the environment and on the pollution caused by human activities [8, 9], being also very important in many industrial technologies [10–13] and in the optimization of combustion processes of the fossil fuels [14, 15].

Many theoretical studies [16–19] and experimental investigations [20–26] on the electron-NO reactions are available and recently reviewed by Song *et al* [27] and by McConkey
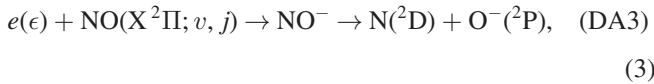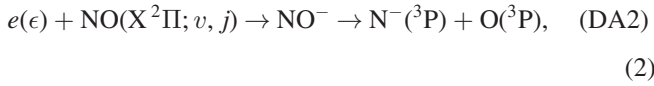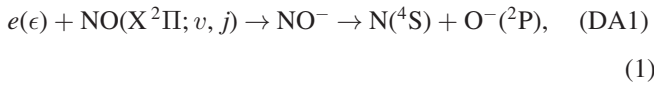
et al [28]. Specifically, concerning the DA process, the theoretical studies are limited to very low scattering energy and to the few lowest vibrational states corresponding to the ground electronic state of NO, and only few low-lying resonant states of NO⁻ [18] are taken into account. The only absolute experimental DA cross section measurements were performed by Rapp and Briglia [22] who observed O⁻ production from the $v = 0$ vibrational state of NO. Experiments have detected both excited nitrogen atoms and N⁻ production from DA [29–32] but these observations are not yet understood. Moreover, accurate collisional-radiative models of plasmas, which are able to investigate internal energy exchanges, require a state-to-state approach, which consists of cross sections resolved over the internal degrees of freedom for the constituent atoms and molecules [4, 5].

In this letter, we present new calculations of ro-vibrational state-resolved cross sections and the corresponding rate coefficients for the following three resonant DA processes:

$$e(\epsilon) + \mathrm{NO}(X\,^2\Pi; v, j) \rightarrow \mathrm{NO}^- \rightarrow \mathrm{N}(^4\mathrm{S}) + \mathrm{O}^-(^2\mathrm{P}), \quad \text{(DA1)}$$
(1)

$$e(\epsilon) + \mathrm{NO}(X\,^2\Pi; v, j) \rightarrow \mathrm{NO}^- \rightarrow \mathrm{N}^-(^3\mathrm{P}) + \mathrm{O}(^3\mathrm{P}), \quad \text{(DA2)}$$
(2)

$$e(\epsilon) + \mathrm{NO}(X\,^2\Pi; v, j) \rightarrow \mathrm{NO}^- \rightarrow \mathrm{N}(^2\mathrm{D}) + \mathrm{O}^-(^2\mathrm{P}), \quad \text{(DA3)}$$
(3)

where v and j represent the vibrational and rotational quantum number of the NO molecule. In the following, where not explicitly specified, we assume $j = 0$; rotational effects are discussed in the last part of the letter. Since the excited electronic states of nitrogen atoms as well as its negative ion are unstable they undergo decays toward the ground state N(⁴S): in the plasma, the reaction DA2 will be followed by detachment process by electron emission for N⁻ [33] and DA3 channel will be followed by radiative decay to N(²D).

As specified in [1], in order to cover a large energy range for the incident electron, we take into account five resonant electronic states of NO⁻: three low-lying—*i.e.* of $^3\Sigma^-$, $^1\Sigma^+$ and $^1\Delta$ symmetries—and two higher—of $^3\Pi$ and $^1\Pi$ symmetries—close to the NO dissociation threshold. In the following, we will refer to these resonances by $r = 1, \ldots, 5$. The correspondence between each resonance r and a specific channel $i = 1, 2, 3$, associated to an asymptotic (dissociation) limit, is reported in table 1, which also gives the electron affinity for each process.

According to the theoretical formalism of the local-complex-potential (LCP)—previously used to study the NO dissociative excitation process in [1] and the DA of O₂ [34]—the DA cross section for an NO molecule initially in its vibrational level v colliding with an electron of incident energy ϵ and following channel i is given by [35]:

$$\sigma_v^i(\epsilon) = \sum_r \frac{2S_r + 1}{(2S+1)}\frac{g_r}{2\,g}\,2\pi^2\,\frac{K}{\mu}\,\frac{m_e}{k}\lim_{R\to\infty}\left|\xi_v^r(R)\right|^2, i = 1,2,3,$$
(4)

Table 1. Asymptotic limit positions of the NO⁻ resonant states considered in the calculations for the three DA channels (1)–(3). The energy is expressed with respect to the asymptotic limit of the ground electronic state of NO. Experimental energy values, from Mazeau *et al* [33] and NIST database [38], are given in brackets for comparison. The last column reports the correlation with the resonances for each channel.

Channel	Limit	Energy (eV)	Symmetries
DA1	N(⁴S) + O⁻(²P)	−1.460 (−1.46)	$^3\Sigma^-$
DA2	N⁻(³P) + O(³P)	+0.068 (+0.07)	$^1\Delta, {}^1\Sigma^+$
DA3	N(²D) + O⁻(²P)	+0.910 (+0.91)	$^3\Pi, {}^1\Pi$

where $2S_r + 1$ and $2S + 1$ are the spin-multiplicities of the resonant electronic state of the anion and of the electronic state of the neutral target, respectively, g_r and g represent the corresponding degeneracy factors, K is the asymptotic momentum of the final dissociating fragments, k is the incoming electron momentum, μ is the reduced mass of NO nuclei, m_e is the electron mass and ξ_v^r is the resonant wave function solution of the nuclear equation with total energy $E = \epsilon_v + \epsilon$:

$$\left[-\frac{\hbar^2}{2\mu}\frac{d^2}{dR^2} + V_r^-(R) - \frac{i}{2}\Gamma_r(R) - E\right]\xi_v^r(R)$$
$$= -\mathcal{V}_r(R)\,\chi_v(R), \quad r = 1, \ldots, 5. \quad (5)$$

In equation (5), V_r^- and Γ_r represent the potential energies and the autoionization widths, respectively, for the five resonant NO⁻ states included in the calculation, $\mathcal{V}_r$ the discrete-to-continuum coupling defined in [1] and χ_v is the wave function of the initial vibrational state of NO with energy ϵ_v:

$$\left[-\frac{\hbar^2}{2\mu}\frac{d^2}{dR^2} + V_0(R)\right]\chi_v(R) = \epsilon_v\,\chi_v(R), \quad (6)$$

where V_0 is the potential energy of the ground electronic state of NO(X²Π). Full details concerning the LCP theoretical model are reported in [1] and in the seminal papers [35–37].

Figure 1 reports the complete set of potential energy curves for NO in its ground electronic state, and the five NO⁻ resonances and their corresponding autoionization widths. A discussion on molecular data determination as well as all input parameters entering in the equations (4)–(6) can be found in [1]. In order to validate the resonance widths used in the present work and in [1], comparison with *ab initio* Kohn variation principle results available in the paper [19] are shown in figure 2. Table 2 contains the list of the vibrational levels v supported by the NO molecule in its ground rotational state, *i.e.* $j = 0$.

Figures 3–6 contain the results of this letter. In order to validate the theoretical model, figure 3 reports the comparison between the calculated DA cross section for $v = 0$ with the experimental data of Rapp and Briglia [22]. The global agreement is quite satisfactory. Looking in detail, we note that the low energy contribution comes from the DA1 channel, which corresponds to the N(⁴S) + O⁻(²P) fragments, both in the ground electronic state, and when the DA3 channel opens, around 7.5 eV, the cross section is dominated by the production of the excited nitrogen atom N(²D) and of the anion O⁻(²P).
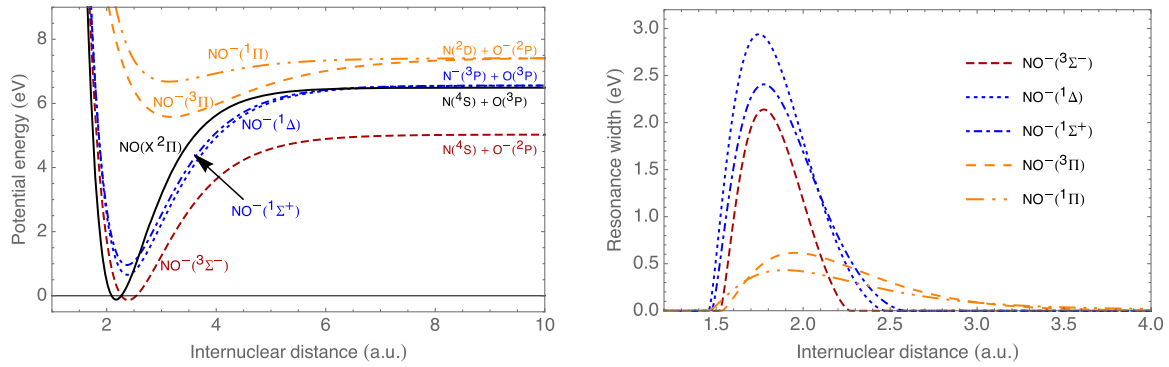
Figure 1. Molecular data as determined in [1]. Left: potential energy curves for the ground electronic state of NO molecule (solid line) and for the five NO^- resonances (broken lines) included in the calculations, for $j = 0$; right: the corresponding widths of the resonances.
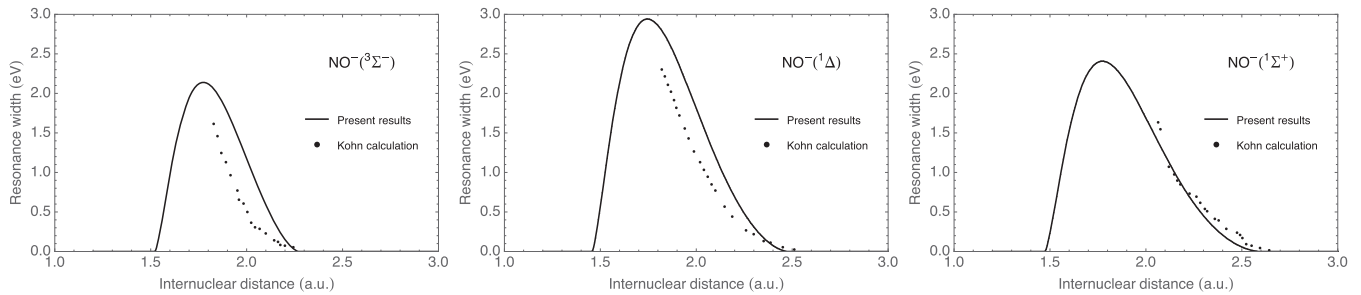

Figure 2. Autoionization widths of the low-lying NO^- resonances: comparison of the values used in the present calculation with those coming from the Kohn computations [19].

Table 2. Energies of the vibrational levels of the electronic ground state of the NO molecule for $j = 0$. The dissociation energy for the ground vibrational level is $D_0 = 6.490$ eV.

v	ϵ_v (eV)	v	ϵ_v (eV)	v	ϵ_v (eV)
0	0.000	18	3.581	36	5.745
1	0.236	19	3.739	37	5.823
2	0.468	20	3.892	38	5.897
3	0.695	21	4.040	39	5.967
4	0.918	22	4.185	40	6.033
5	1.137	23	4.324	41	6.094
6	1.351	24	4.460	42	6.150
7	1.561	25	4.591	43	6.203
8	1.767	26	4.718	44	6.251
9	1.968	27	4.840	45	6.294
10	2.164	28	4.958	46	6.333
11	2.357	29	5.072	47	6.368
12	2.545	30	5.181	48	6.399
13	2.729	31	5.286	49	6.425
14	2.908	32	5.386	50	6.446
15	3.083	33	5.483	51	6.464
16	3.253	34	5.574	52	6.477
17	3.419	35	5.662	53	6.485

Figure 3. O^- production from DA1 and DA3 processes for $v = 0$: comparison of the present calculations for $j = 0$ with the experimental data of Rapp and Briglia [22].

section for NO given in [29, 30] and with the experimental observations reported in [31].

Figure 4 displays the cross sections branching ratios (BR) for some initial vibrational states v. They are defined by:

$$\mathrm{BR}_v^i(\epsilon) = \frac{\sigma_v^i(\epsilon)}{\sum_{j=1}^{3} \sigma_v^j(\epsilon)}, \quad i = 1, 2, 3, \tag{7}$$

where i stands for the channel. In general, for all values of v, the DA1 and DA3 channels provide the major contributions to the reaction products. In particular, DA1 dominates the cross

The contribution coming from the DA2 channel is negligible: indeed, the electron affinity of the nitrogen atom is positive and very small—see table 1—and, on the other hand, for low vibrational levels the production of N^- is energetically forbidden. This is consistent with the interpretation of the DA cross
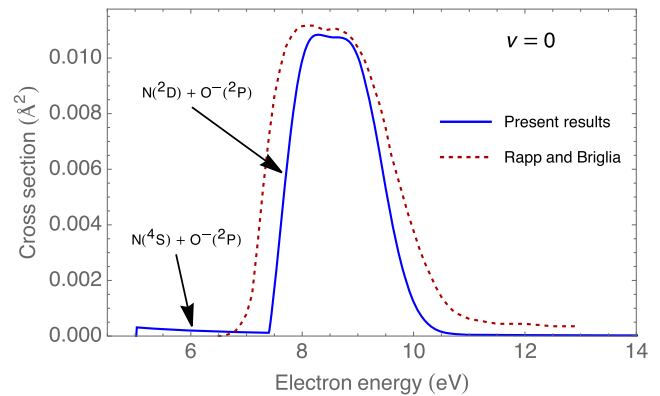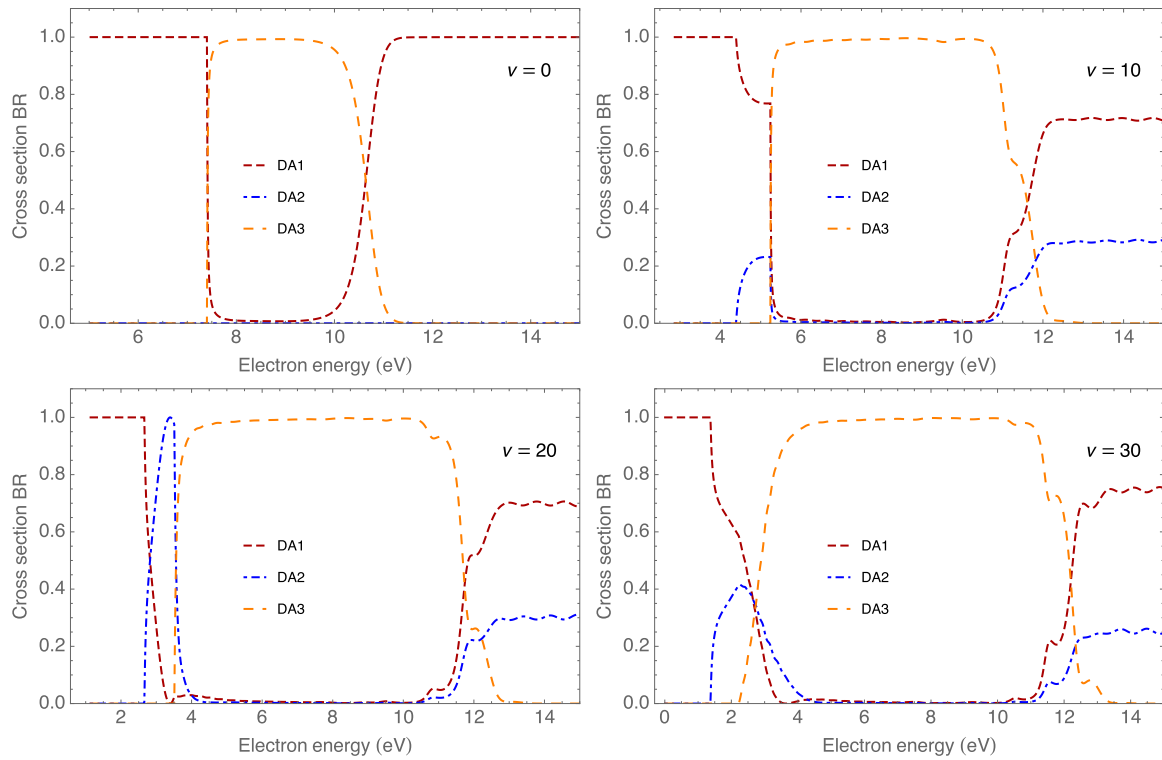
Figure 4. Cross section BR for the three DA channels in (1)–(3) for $v = 0$, $v = 10$, $v = 20$ and $v = 30$, for $j = 0$.
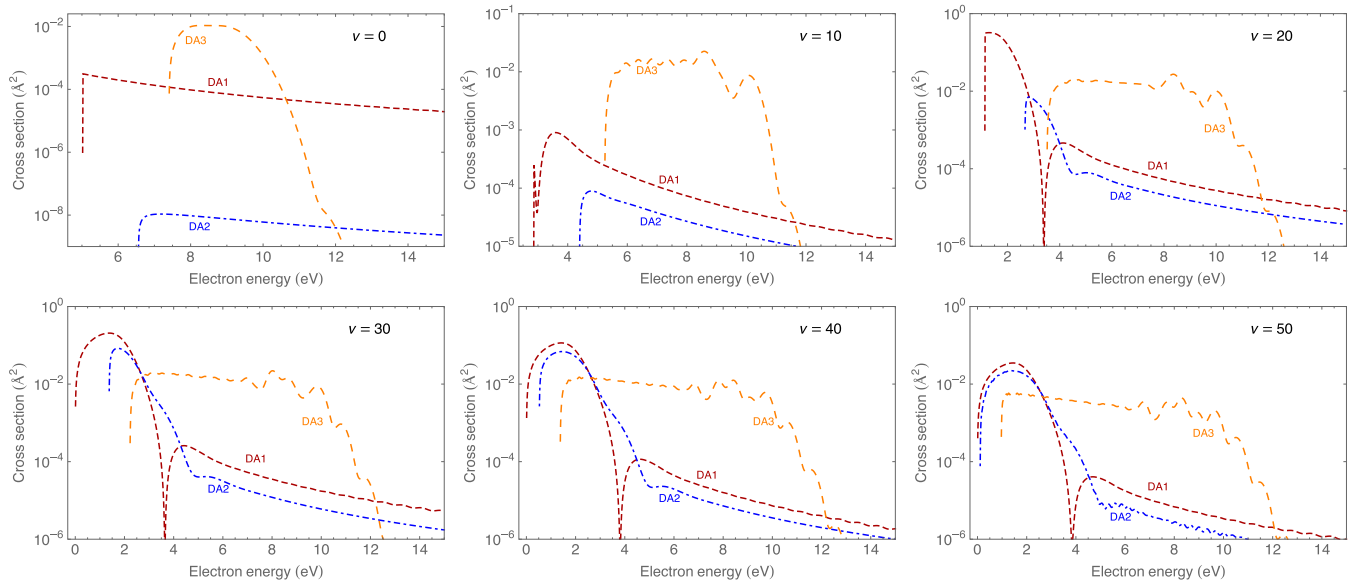

Figure 5. Overview over vibrational- and channel-resolved cross sections for NO dissociative electron attachment process for $j = 0$.

section at low and at high energies, whereas DA3 is important at intermediate energies. This is due to an interplay of two factors: (i) the DA3 threshold is higher than the DA1 one and, as a consequence, this latter channel dominates at low energies; (ii) the resonance/autoionization continuum couplings within the $^3\Pi$ and the $^1\Pi$ symmetry are smaller than those within the $^3\Sigma^-$ symmetry, and they are confined to a narrow energy range around the DA3 threshold, meaning that the contribution of the channel (3) drops off quickly at higher energy.

The DA2 channel becomes more prominent as the NO vibrational level, v, increases. The importance of the DA2 channel depends on energy as does that of the DA1 one, as a consequence of the similarity of the couplings characterizing the states to which they are correlated—see rhs of figure 1. The DA2 contribution becomes evident close to the N^- threshold and at high energies: in general its contribution ranges from 20% to 40% of the total cross section. In particular, for $v = 20$, we notice an enhancement of the BR close to 3 eV, where the
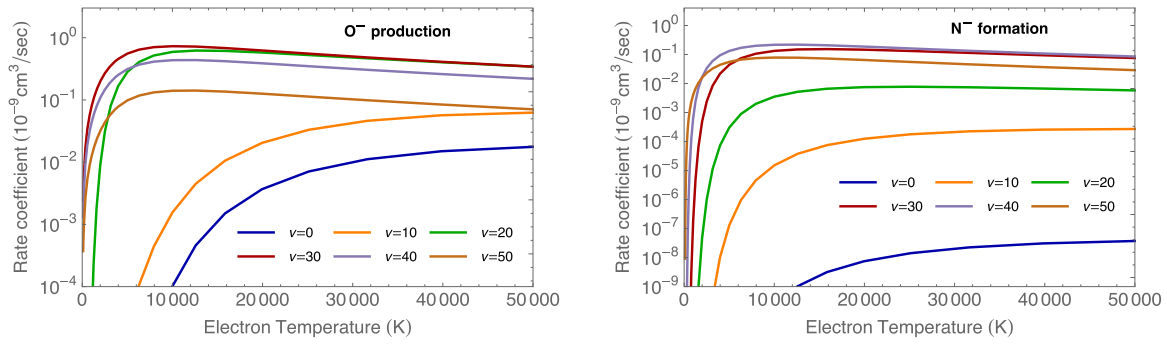
4

Figure 6. Summary on vibrational state-resolved rate coefficients for NO dissociative electron attachment process: on the left side, O⁻ production sum over DA1 and DA3 channels; on the right side, N⁻ formation coming from DA2 channel.
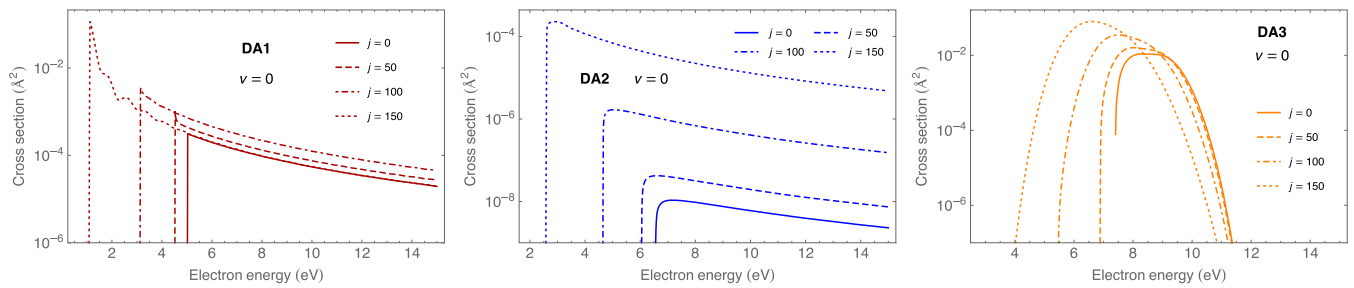

Figure 7. Effects of molecular rotation on cross sections for $v = 0$.

Franck-Condon factors are particularly favorable, and where the DA2 channel becomes dominant in the DA of NO and, consequently, in the production of N⁻ anions.

Figure 5 provides an overview of our vibrational–and channel-resolved absolute cross sections for NO dissociative electron attachment. To validate the numerical results, we varied the coefficients in table 1 of [1] by ±10% and found that the effect on the cross sections is negligible. Figure 6 reports the full sets of results for O⁻ production (DA1 and DA3 channels) and for N⁻ formation (DA2 channel)—resolved over the vibrational ladder—for DA rate coefficient K_v, by assuming a Maxwellian distribution for the electrons at temperature T_e:

$$K_v(T_e) = \left(\frac{1}{m\,\pi}\right)^{1/2} \left(\frac{2}{k_B T_e}\right)^{3/2} \int \epsilon\, \sigma_v(\epsilon)\, e^{-\epsilon/k_B T_e}\, d\epsilon. \quad (8)$$

Since three channels contribute to the full cross section, and the dissociative paths open at different thresholds, the trend of the rate coefficient as a function of the vibrational level v is not regular.

Finally, figure 7 shows the effects of molecular rotation on the cross sections for the three channels DA1, DA2 and DA3, for $v = 0$. As expected, for all three processes, rotational excitation generates a threshold-shift in the curves toward smaller energies: this behavior is, basically, due to the fact that the depth of the potential well decreases as the rotational quantum number j increases and accordingly the corresponding channel open earlier. The calculated rotationally excited cross sections are essentially insensitive to j at high energies for DA1 and DA3 channels, whereas the DA2 process exhibit a large rotational effect and the whole cross section increases

by several order of magnitude as a function of j. The reasons for this behavior can be traced back to the shape of the effective potentials for $j > 0$ compared to that for $j = 0$ and in particular on the relative positions of the NO⁻ asymptotes compared to the NO asymptote: for the DA2 process the NO⁻($^1\Delta$), and NO⁻($^1\Sigma^+$) thresholds are very close to the NO threshold, the effective potentials for $j > 0$ are a 'compressed-copy' of the $j = 0$ one and this drives an enhancement in the cross sections—i.e. same shape but at higher energies. Conversely, rotational excitation distorts the shape of the effective potentials and this effect disappears.

In conclusion, in this letter we presented ro-vibrational state-resolved cross sections of the dissociative electron attachment process for the nitric oxide computed by using the theoretical formalism of the LCP. We focused on three different channels of scattering (1–3), which result in the production of excited nitrogen atoms and of N⁻ anions. The principal results can be outlined as follows:

(a) The major contribution to the experimental DA cross section for $v = 0$ is due to the production of nitrogen atoms in the excited state N(^{2}D);

(b) An important amount of N⁻ ions is produced in the DA of vibrationally excited NO molecules;

(c) Large rotational effects are found in particular for DA2 channel where the corresponding cross section increases by several orders of magnitude compared to that for $j = 0$.

The full set of data obtained in the present work and in [1] are available from the LXCat database (www.lxcat.net/Laporta) [39].

ORCID iDs

V Laporta ⬡ https://orcid.org/0000-0003-4251-407X
I F Schneider ⬡ https://orcid.org/0000-0002-4379-1768
J Tennyson ⬡ https://orcid.org/0000-0002-4994-5238

References

[1] Laporta V, Tennyson J and Schneider I F 2020 *Plasma Sources Sci. Technol.* **29** 05LT02
[2] Campbell L, Brunger M J, Petrovic Z L, Jelisavcic M, Panajotovic R and Buckman S J 2004 *Geophys. Res. Lett.* **31**
[3] Munafò A, Lani A, Bultel A and Panesi M 2013 *Phys. Plasmas* **20** 073501
[4] Annaloro J and Bultel A 2014 *Phys. Plasmas* **21** 123512
[5] Heritier K L, Jaffe R L, Laporta V and Panesi M 2014 *J. Chem. Phys.* **141** 184302
[6] Laporta V and Bruno D 2013 *J. Chem. Phys.* **138** 104319
[7] Laporta V, Heritier K L and Panesi M 2016 *Chem. Phys.* **472** 44
[8] Kreuzer L B and Patel C K N 1971 *Science* **173** 45
[9] Spicer C W 1967 *Atmos. Environ.* **11** 1089
[10] Campbell L and Brunger M J 2016 *Int. Rev. Phys. Chem.* **35** 297
[11] Campbell L and Brunger M J 2012 *Plasma Sources Sci. Technol.* **22** 013002
[12] Motapon O *et al* 2006 *Plasma Sources Sci. Technol.* **15** 23
[13] Barth C A, Mankoff K D, Bailey S M and Solomon S C 2003 *J. Geophys. Res.: Space Phys.* **108** 1027
[14] Slavchov R I, Salamanca M, Russo D, Salama I, Mosbach S, Clarke S M, Kraft M, Lapkin A A and Filip S V 2020 *Fuel* **267** 117218
[15] Lavoie G A, Heywood J B and Keck J C 1970 *Combust. Sci. Technol.* **1** 313
[16] de Vivie R and Peyerimhoff S D 1988 *J. Chem. Phys.* **89** 3028
[17] Laporta V, Celiberto R and Wadehra J M 2012 *Plasma Sources Sci. Technol.* **21** 055018
[18] Trevisan C S, Houfek K, Zhang Z, Orel A E, McCurdy C W and Rescigno T N 2005 *Phys. Rev.* A **71** 052714
[19] Zhang Z, Vanroose W, McCurdy C W, Orel A E and Rescigno T N 2004 *Phys. Rev.* A **69** 062711
[20] Chantry P J 1968 *Phys. Rev.* **172** 125
[21] Allan M 2005 *J. Phys. B: At. Mol. Opt. Phys.* **38** 603
[22] Rapp D and Briglia D D 1965 *J. Chem. Phys.* **43** 1480
[23] Jelisavcic M, Panajotovic R and Buckman S J 2003 *Phys. Rev. Lett.* **90** 203201
[24] Josic L, Wróblewski T, Petrovic Z L, Mechlinska-Drewko J and Karwasz G P 2001 *Chem. Phys. Lett.* **350** 318
[25] Krishnakumar E and Srivastava S K 1988 *J. Phys. B: At. Mol. Opt. Phys.* **21** L607
[26] Van Brunt R J and Kieffer L J 1974 *Phys. Rev.* A **10** 1633
[27] Song M-Y, Yoon J-S, Cho H, Karwasz G P, Kokoouline V, Nakamura Y and Tennyson J 2019 *J. Phys. Chem. Ref. Data* **48** 043104
[28] McConkey J W, Malone C P, Johnson P V, Winstead C, McKoy V and Kanik I 2008 *Phys. Rep.* **466** 1
[29] Sambe H and Ramaker D E 1991 *J. Chem. Phys.* **94** 2548
[30] Orient O J and Chutjian A 1995 *Phys. Rev. Lett.* **74** 5017
[31] Nandi D, Prabhudesai V S, Nestmann B M and Krishnakumar E 2011 *Phys. Chem. Chem. Phys.* **13** 1542
[32] Denifl G, Muigg D, Stamatovic A and Märk T D 1998 *Chem. Phys. Lett.* **288** 105
[33] Mazeau J, Gresteau F, Hall R I and Huetz A 1978 *J. Phys. B: At. Mol. Phys.* **11** L557
[34] Laporta V, Celiberto R and Tennyson J 2015 *Phys. Rev.* A **91** 012701
[35] Dubé L and Herzenberg A 1979 *Phys. Rev.* A **20** 194
[36] Bardsley J N and Mandl F 1968 *Rep. Prog. Phys.* **31** 471
[37] Domcke W 1991 *Phys. Rep.* **208** 97
[38] Kramida A, Ralchenko Y, Reader J and NIST ASD Team 2018 *NIST Atomic Spectra Database (Ver. 5.5.2)* (Gaithersburg, MD: National Institute of Standards and Technology) available online: https://physics.nist.Gov/asd [2018, January 30]
[39] Pitchford L C *et al* 2017 *Plasma Process. Polym.* **14** 1600098